

Characterization and Correction of Physiological Instabilities in 3D FMRI

R. H. Tijssen¹, S. M. Smith¹, P. Jezzard¹, R. Frost¹, M. Jenkinson¹, and K. L. Miller¹

¹FMRIB Centre, Oxford University, Oxford, Oxon, United Kingdom

Introduction.

3D readouts generally have the advantage that they 1) allow imaging at a high isotropic resolution and 2) are inherently multi-shot sequences with short readout segments thereby reducing distortion artifacts. These advantages make sequences such as steady-state free-precession (SSFP) and spoiled gradient echo (SPGR) an attractive option for high resolution FMRI in areas such as the brainstem. Experiments have shown however that these sequences are prone to temporal instabilities in inferior areas of the brain (Fig. 1). In this work we present a characterisation of these instabilities by simulations and report preliminary results of a GRAPPA-based correction method that utilizes the additional information of the coil geometry to allow retrospective gating of 3D FMRI data.

Methods. Data acquisition. 2D and 3D balanced SSFP data were acquired on a 3T Siemens scanner (Siemens, Erlangen) using a 12-channel head coil. For the 2D data, single coronal slices (resolution= $2 \times 2 \times 2.5$ mm) were acquired every 152ms (2000 volumes) to critically sample the respiratory and cardiac waveforms (for scan parameters see [1]). This 2D data was used to simulate the effects of physiological noise on 3D acquisitions. The 3D data were acquired using a 'stack of segmented EPI' readout [2]. Scan parameters were: $\alpha=30^\circ$, $T_R/T_E=9/4.6$ ms, 1860 Hz/pix, 8 lines per T_R , resolution= 2×2 , matrix= $96 \times 88 \times 24$, no acceleration. For both data sets heart and respiration waveforms were recorded, as well as scanner triggers to synchronize the data with the image acquisition.

Simulations using the 2D timeseries were performed to investigate the source of the signal instabilities seen in the 3D data. Artificial 3D k-space was generated from the 2D k-space timeseries by concatenating 2D k-space matrices from consecutive time points to form the third dimension (k_z). For a temporally stable signal, this simulated 3D k-space corresponds to a single slice in image space and no signal outside this slice. In the presence of temporal instability, the signal will fluctuate along the simulated third dimension, and introduce dispersed signal into adjacent slices. This is the hypothesized source of increased signal instabilities present in 3D acquisitions. We used this framework to investigate the effect of the respiratory and cardiac cycles. We investigated two types of corrections. First, rejection of data acquired during systole; and second the effect of reordering the data to achieve a smooth variation of the respiratory or cardiac cycle across k-space.

Corrections on real data. Based on our simulations, we investigated a practical method for discarding data acquired during systole without affecting the frame rate in an FMRI experiment. The multi-channel raw data for the 3D acquisition was retrospectively synchronized to the cardiac triggers. For each volume the k-space segments that were acquired during systole were rejected. A parallel-imaging approach was then used to fill in the missing lines and reconstruct the final images. This reconstruction utilized a GRAPPA kernel [3] to estimate ("fill in") the rejected segments for each k-space volume.

Results and Discussion. Figure 1 shows the improved temporal stability of 2D SSFP compared to 2D GRE-EPI, which is one of the motivations for using SSFP FMRI in areas that are prone to physiological noise such as the brainstem. For the 3D variant the temporal signal-to-noise (tSNR) is further improved in cortical regions, which can be attributed to the increased available signal in 3D readouts. For regions around the ventricles and the brainstem, on the other hand, the tSNR is considerably reduced. This is likely due to phase offsets between the readout segments caused by CSF pulsation and vascular motion, which can cause the signal to be 'remapped' incorrectly in image space. This is confirmed by our simulations, which show a significant amount of signal fluctuations in slices outside the central slice (slice 8), which contains the image (Fig. 2, top row). The difference maps show that less signal is dispersed into the slices outside the central slice when data acquired during systole is discarded (middle row). The fluctuations are further reduced when cardiac gating is combined with reordering of the data with respect to the cardiac cycle (bottom row). Figure 3 shows the initial results of the proposed correction method. As predicted by our simulations, an increase in the stability is seen in the areas that are most prone to signal fluctuations (e.g. CSF regions and major arteries). At this stage a standard grappa approach is used estimate the rejected lines in k-space, which may explain the overall reduced stability in the cortical regions. It is believed that optimization of the GRAPPA reconstruction will mitigate these effects, which is a topic of ongoing research.

Conclusions. We have shown that post-hoc cardiac gating has the ability to increase the temporal stability by discarding the lines in k-space that were acquired during systole. A GRAPPA reconstruction was employed to fill in the missing lines. This has the advantage that the time volume acquisition remains constant, which is beneficial for FMRI. Our simulations indicate that further improvements in temporal stability should be achievable by re-ordering k-space acquisition such that the cardiac cycle varies smoothly across k-space. Future work will investigate this possibility by using real-time processing to synchronize acquisition to cardiac triggers.

References. [1] Tijssen et al. ISMRM 2009 p. 1591 [2] Miller et al. MRM 2006;55(1)151-170 [3] Griswold et al. MRM, 47(6):1202-1210, 2002.

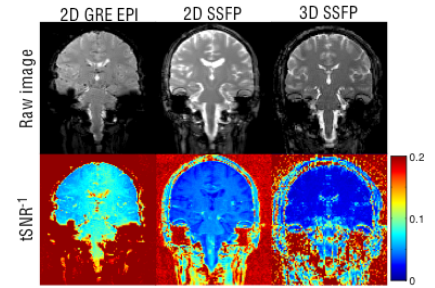


Figure 1: Images acquired with 2D GRE-EPI, 2D SSFP and 3D SSFP (top) and their corresponding tSNR⁻¹ maps (bottom).

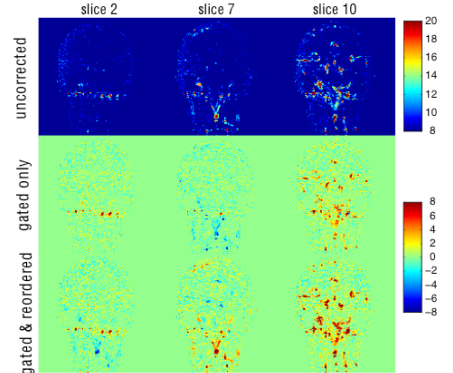


Figure 2: Simulation results showing the temporal SD outside the central slice (top). The middle and bottom figure show the difference between the temporal SD of the uncorrected and the gated versions of the data. Red denotes improvement and blue worsening of the temporal stability.

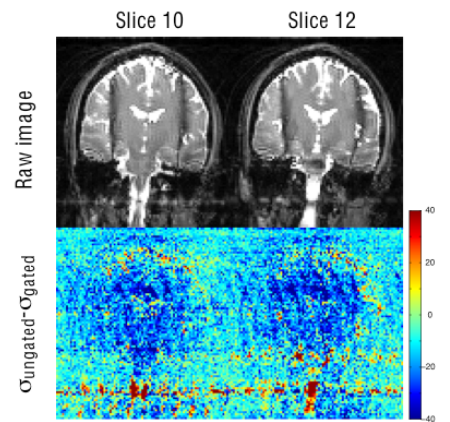


Figure 3: Correction results showing the difference in temporal variability between the corrected and uncorrected data sets. Red denotes improvement and blue worsening of the temporal stability.